Scattering from Artificial Piezoelectriclike Meta-Atoms and Molecules

Leonid Goltcman and Yakir Hadad*
School of Electrical Engineering, Tel-Aviv University, Ramat-Aviv, Tel-Aviv 69978, Israel

(Received 6 September 2017; published 30 January 2018)

Inspired by natural piezoelectricity, we introduce hybrid-wave electromechanical meta-atoms and metamolecules that consist of coupled electrical and mechanical oscillators with similar resonance frequencies. We explore the linearized electromechanical scattering process and demonstrate that by exploiting the hybrid-wave interaction one may enable functionalities that are forbidden otherwise. For example, we study a dimer metamolecule that is highly directional for electromagnetic waves, although it is electrically deep subwavelength. This unique behavior is a consequence of the fact that, while the metamolecule is electrically small, it is acoustically large. This idea opens vistas for a plethora of exciting dynamics and phenomena in electromagnetics and acoustics, with implications for miniaturized sensors, superresolution imaging, compact nonreciprocal antennas, and more.

DOI: 10.1103/PhysRevLett.120.054301

Introduction.—The direction of arrival of an incoming wave can be estimated using the phase difference between the received signal at two adjacent antennas separated by a distance D; this establishes the basic direction-of-arrival sensor. Its sensitivity is maximized when D is set to be half of the wavelength at the desired frequency and severely deteriorates as D becomes subwavelength [1,2]. This is another consequence of the diffraction limit [3] that imposes stringent constraints on the resolution of far-field imaging. In recent years, metamaterials have acquired a reputation for achieving effective material functionalities that do not exist in nature [4,5] and for violating fundamental bounds, such as due to time-reversal symmetry [6–12]. In this Letter, we propose a paradigm of hybrid-wave electromechanical metamaterial that can create a synthetic sense of length and, thus, effectively transform an electrically small structure to behave as if it is electrically large. Hybrid-physics metamaterials have already been explored for several purposes, for instance, to create real time reconfigurable and tunable devices [13,14], utilizing thermal [15,16], electrostatic [17–19], magnetic [20], and optical [21–23] actuation. In a different context, hybrid-physics optomechanical crystalline structures, known as phoxonic crystals [24], have been proposed as a means to achieve strong nonlinear photon-phonon interactions via simultaneous infrared-photonic and gigahertz-phononic Bragg resonances. These and similar optomechanical structures have been proposed for nonlinear metamaterials [25], tunable gigahertz resonators [26–28], quantum processing [27,28], and as a means for studying many-body dynamics [29–31], as well as for long-range synchronization [32]. Recently, the inherent nonlinearity of cavity optomechanics has been utilized to obtain spontaneous symmetry breaking [33] and magnetless nonreciprocity [34,35]. In contrast to previous work, here, we introduce meta-atoms that involve hybridization of electromagnetic and acoustic resonances at the same frequency and in a linearizable configuration. After modeling the electromechanical scattering process, we show that by clustering metamolecules one may enable functionalities that are forbidden otherwise. As an example, we design an electrically deep subwavelength, but highly directional, dimer metamolecule sensor.

The electromechanical meta-atom.—Wave scattering typically occurs within one physical realm, such as in the cases of electromagnetic scattering, acoustic scattering, elastic scattering, etc. Here, however, we consider a hybrid-physics scattering. An electromechanical (EMCL) scatterer partially transforms an impinging electromagnetic $\mathbf{E}^i$ or acoustic $\mathcal{P}^i$ wave into a mixture of acoustic and electromagnetic scattered waves $\mathbf{E}^s$ and $\mathcal{P}^s$, as illustrated in Fig. 1(a). This type of scattering exists in natural piezoelectric or photoelastic materials; however, it may be better controllable and more

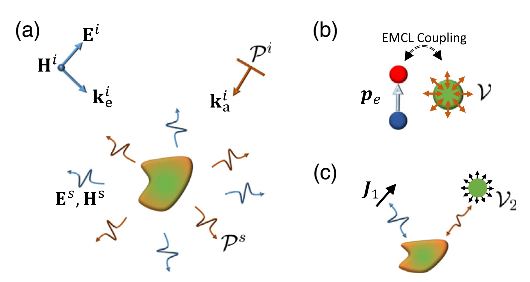

FIG. 1. (a) Illustration of the generalized hybrid-physics scattering process. An electromechanical meta-atom can be excited by both electromagnetic and acoustic fields, and it generally scatters the two types of wave, regardless of the excitation. (b) If the resonators are electrically and acoustically small, they compose a coupled system of an electric dipole and an acoustic monopole. Both radiate to the external ambient surroundings. (c) A configuration in which mutual action between the electric current source $\mathbf{J}_1$ and the acoustic pressure source $\mathcal{V}_2$ takes place via an EMCL meta-atom.

efficient using artificial materials that involve EMCL coupled resonators. Such artificial materials are composed of lattices of EMCL meta-atoms. The latter are excited by and radiate EMCL fields. We define an EMCL field as a four-element vector containing the three electric field components and the scalar pressure field $\mathbf{U}(\mathbf{r}) = [E_x, E_y, E_z, \mathcal{P}]^T$. When an EMCL field impinges on an EMCL meta-atom, electric and acoustic sources are induced, as illustrated in Fig. 1(b). Assuming that the meta-atom is small enough compared to the wavelength of light and sound, the induced sources are appropriately modeled by a coupled electric dipole $\mathbf{p}_e$ and acoustic monopole with volume $\mathcal{V}$ (so that its volume velocity is $\mathcal{U} = \dot{\mathcal{V}}$). These constitute the EMCL source $\mathbf{S} = [p_{ex}, p_{ey}, p_{ez}, \mathcal{V}]^T$. Generally, the coupled EMCL problem is inherently nonlinear; however, we restrict this work to the class of problems that can be linearized under the weak signal assumption. The induced source $\mathbf{S}$ is related to the impinging field $\mathbf{U}$ at the meta-atom location via the linear response matrix,

$$\mathbf{S} = \underline{\underline{\alpha}}\mathbf{U}, \quad \text{with} \quad \underline{\underline{\alpha}} = \begin{bmatrix} \underline{\underline{\alpha}}_{ee} & \underline{\underline{\alpha}}_{ea} \\ \underline{\underline{\alpha}}_{ae} & \underline{\underline{\alpha}}_{aa} \end{bmatrix}. \tag{1}$$

The diagonal terms are the common response terms in the absence of EMCL coupling. Specifically,

$$\underline{\underline{\alpha}}_{ee} = \begin{bmatrix} \alpha_{ee}^{xx} & \alpha_{ee}^{xy} & \alpha_{ee}^{xz} \\ \alpha_{ee}^{yx} & \alpha_{ee}^{yy} & \alpha_{ee}^{yz} \\ \alpha_{ee}^{zx} & \alpha_{ee}^{zy} & \alpha_{ee}^{zz} \end{bmatrix}, \qquad \underline{\underline{\alpha}}_{aa} = \alpha_{aa}, \tag{2}$$

where $\underline{\underline{\alpha}}_{ee}$ is the electric polarizability that describes the induced dipolar moment due to an impinging electromagnetic field and $\underline{\underline{\alpha}}_{aa}$ gives the acoustic monopole volume induced by an impinging pressure field. The off-diagonal, EMCL coupling terms in Eq. (1) read

$$\underline{\underline{\alpha}}_{ea} = [\alpha_{ea}^x, \alpha_{ea}^y, \alpha_{ea}^z]^T, \qquad \underline{\underline{\alpha}}_{ae} = [\alpha_{ae}^x, \alpha_{ae}^y, \alpha_{ae}^z]. \tag{3}$$

These terms are responsible for the direct and reverse piezoelectriclike behavior of the meta-atom. Clearly, if the meta-atom exhibits no practical EMCL coupling, then $\underline{\underline{\alpha}}_{ae} = \underline{\underline{\alpha}}_{ea} = 0$, and, if in addition it is only electric (acoustic), then $\underline{\underline{\alpha}}_{aa} = 0$ ($\underline{\underline{\alpha}}_{ee} = 0$).

Now, closing the loop, the field $\mathbf{U}(\mathbf{r})$ radiated by an induced source $\mathbf{S}$ on a meta-atom at $\mathbf{r}'$ is given by the EMCL Green's function $\mathbf{U}(\mathbf{r}) = \underline{\underline{G}}(\mathbf{r}, \mathbf{r}')\mathbf{S}$. Assuming that there is no EMCL interaction in the ambient medium, $\underline{\underline{G}}$ is block diagonal and reads

$$\underline{\underline{G}}(\mathbf{r}, \mathbf{r}') = \begin{bmatrix} \underline{\underline{G}}_e(\mathbf{r}, \mathbf{r}') & 0 \\ 0 & G_a(\mathbf{r}, \mathbf{r}') \end{bmatrix}, \tag{4}$$

where $\underline{\underline{G}}_e$ (G_a) is the electric dyadic (acoustic scalar) Green's function connecting $\mathbf{p}_e$ ($\mathcal{V}$) to $\mathbf{E}$ ($\mathcal{P}$).

Fundamental constraints on $\underline{\underline{\alpha}}$.—The linear response matrix is subject to fundamental constraints due to reciprocity and energy conservation. We begin with reciprocity. Consider the hypothetical setup in Fig. 1(c) that contains an electric current $\mathbf{J}_1$, an acoustic monopole with volume velocity $\mathcal{U}_2 = \dot{\mathcal{V}}_2$, and an EMCL meta-atom. In the absence of the meta-atom, the interaction between the two sources is obviously zero. However, in the presence of the EMCL meta-atom, the electric field radiated by the current source $\mathbf{J}_1$ impinges on the meta-atom and, consequently, gives rise to scattering of both electromagnetic and acoustic pressure waves. The latter, denoted here by $\mathcal{P}_1$, interacts with the acoustic source $\mathcal{U}_2$, implying that this time an action $\mathcal{A}[\mathbf{J}_1 \to \mathcal{U}_2] = \mathcal{P}_1\mathcal{U}_2$ between the sources takes place. In the reciprocal scenario, the acoustic source $\mathcal{U}_2$ acts on $\mathbf{J}_1$ through the scattered electromagnetic field $\mathbf{E}_2$, $\mathcal{A}[\mathcal{U}_2 \to \mathbf{J}_1] = \mathbf{E}_2 \cdot \mathbf{J}_1$. Since we deal with a linearized system, the mutual action between the sources should be equal [36]:

$$\mathcal{A}[\mathbf{J}_1 \to \mathcal{U}_2] = \mathcal{A}[\mathcal{U}_2 \to \mathbf{J}_1]. \tag{5}$$

Expressing Eq. (5) using the electromagnetic and acoustic Green's functions, we find [37]

$$\begin{aligned} &\mathcal{U}_2 G_a(\mathbf{r}_2, \mathbf{r}_s)\underline{\underline{\alpha}}_{ae}\underline{\underline{G}}_e(\mathbf{r}_s, \mathbf{r}_1)\mathbf{J}_1 \\ &= \mathbf{J}_1^T \underline{\underline{G}}_e(\mathbf{r}_1, \mathbf{r}_s)\underline{\underline{\alpha}}_{ea} G_a(\mathbf{r}_s, \mathbf{r}_2)\mathcal{U}_2. \end{aligned} \tag{6}$$

Assuming that the medium is electromagnetically and acoustically reciprocal, $\underline{\underline{G}}_e(\mathbf{r}, \mathbf{r}') = \underline{\underline{G}}_e^T(\mathbf{r}', \mathbf{r})$ [2] and $G_a(\mathbf{r}, \mathbf{r}') = G_a(\mathbf{r}', \mathbf{r})$ [36]. Then, using Eq. (6), we find

$$\underline{\underline{\alpha}}_{ea} = \underline{\underline{\alpha}}_{ae}^T. \tag{7}$$

This symmetry is a manifestation of the principle of microscopic reversibility [38,39] applied to the linearized meta-atom system.

Next, we consider energy conservation. In the absence of material losses of any kind, the power that an impinging EMCL field $\mathbf{U}$ extracts for the excitation of the induced source $\mathbf{S}$ on the meta-atom is equal to the total EMCL power radiated by the meta-atom. The extracted EMCL power reads $P^{\text{ext}} = (\omega/2)\text{Im}\{\mathbf{U}^H\underline{\underline{\alpha}}^H\mathbf{U}\}$, where the superscript H denotes the Hermitian transpose [37]. On the other hand, the total radiated power reads $P^{\text{rad}} = \mathbf{U}^H\underline{\underline{\alpha}}^H\underline{\underline{\chi}}\,\underline{\underline{\alpha}}\mathbf{U}$ with $\underline{\underline{\chi}} = \text{diag}[\underline{\underline{I}}_{3\times3}P_e^{\text{rad}}, P_a^{\text{rad}}]$, where $\underline{\underline{I}}_{3\times3}$ is the 3 by 3 unitary matrix and P_e^{rad} and P_a^{rad}, respectively, are the total powers radiated by an electromagnetic dipole and an acoustic monopole, both of unit amplitudes [37]. For a meta-atom embedded in a homogenous medium with permittivity and permeability ϵ and μ, respectively, and with density ρ_0, we have $P_e^{\text{rad}} = \mu\omega^4/12\pi c_e$ [1] and $P_a^{\text{rad}} = \rho_0\omega^4/8\pi c_a$ [40], where c_e and c_a are, respectively, the speed of light and of sound in the medium. If the medium is more complex, the radiation terms should be corrected accordingly. For instance, for a meta-atom embedded in an electromagnetically transparent, acoustic hard-wall duct with cross section area A_d that supports only a plane wave mode, we have $P_a^{\mathrm{rad}} = \rho\omega^2 c_a/4A_d$ [40], while P_e^{rad} remains unchanged. By equating $P^{\mathrm{ext}} = P^{\mathrm{rad}}$, we find that $\underline{\underline{\alpha}}$ is subject to

$$\underline{\underline{\alpha}}^H \underline{\underline{\chi}}\,\underline{\underline{\alpha}} = (\omega/4j)[\underline{\underline{\alpha}}^H - \underline{\underline{\alpha}}]. \tag{8}$$

This is a generalization of the optical theorem [2–4].

Schematic realization of an EMCL meta-atom.—Consider a parallel plate capacitor with nominal capacitance C_0 loaded by an inductor L to establish an electromagnetic resonance at frequency $\omega_e = 1/\sqrt{LC_0}$. Simultaneously, each capacitor plate acts as a membrane that mechanically resonates at $\omega_m = \sqrt{k/m}$, where m and k are the membrane's effective mass and stiffness, respectively. We assume that the capacitor volume between the plates is acoustically closed, and thus it responds mechanically to external pressure changes. See Fig. 2(a) for an illustration. The system is set at equilibrium by applying a biasing voltage V_0, leading to static charge accumulation, q_0 and $-q_0$, and, thereby, to a constant Coulomb attraction force between the plates. In the absence (presence) of the static biasing, the spacing between the plates is d $(d - x_0)$. Neglecting edge effects, we define the nominal capacitance as $C_0 = \epsilon_c A/(d - x_0)$, where ϵ_c is the permittivity between the plates and A is the plate area.

The meta-atom can be excited by either an electromagnetic or an acoustic wave, as illustrated in Fig. 2(a). Using the concept of effective length in the antenna theory [1], the impinging electromagnetic wave excitation is modeled by a lumped voltage source, $v(t) = l_{\mathrm{eff}} E_x^i(t)$. Here, E_x^i is the electric field component normal to the plates and l_{eff} is the effective length of the capacitor when viewed as an electrically small antenna. Once excited, the meta-atom can be described effectively by an electric dipole $\mathbf{p}_e = p_e\hat{x}$ with $p_e = l_{\mathrm{eff}}\delta q$, coupled to an acoustic monopole with volume $\mathcal{V} = A\delta x$ (volume velocity $\mathcal{U} = \dot{\mathcal{V}} = A\dot{\delta x}$) [36].

The electromechanical dynamics is inherently nonlinear [37]. However, if the excitation is weak enough compared to static biasing so that $\delta q \ll q_0$, then the meta-atom response can be linearized around its equilibrium:

$$\ddot{\delta q} + 2\tau_e^{-1}\dot{\delta q} + \omega_e^2\delta q = L^{-1}[v(t) + E_0\delta x], \tag{9a}$$

$$\ddot{\delta x} + 2\tau_m^{-1}\dot{\delta x} + \omega_m^2\delta x = m^{-1}[f(t) + E_0\delta q]. \tag{9b}$$

Here τ_e^{-1} and τ_m^{-1} are the electromagnetic and mechanical decay rates, respectively, that include radiation, as well as material damping, ω_e and ω_m are as defined earlier, and $E_0 = -V_0/(d - x_0)$ is the static electric field between the capacitor plates. The coupling terms in Eqs. (9) have a clear physical meaning. In Eq. (9a), the small signal deflection δx yields, effectively, an extra voltage source $E_0\delta x$, and, in Eq. (9b), the small signal charge δq creates an extra force between the plates $E_0\delta q$.

The charge fluctuations δq create an effective electric dipolar moment $p_e = l_{\mathrm{eff}}\delta q$, normal to the capacitor plates (along $\hat{x}$). Moreover, the displacement fluctuations δx give rise to an effective acoustic monopole source with volume oscillation amplitude $\mathcal{V} = A\delta x$ and volume velocity $\mathcal{U} = j\omega\mathcal{V}$ (here and henceforth, time dependence $e^{j\omega t}$ is assumed and suppressed). Finally, the system's linear response is expressed in the form of Eq. (1), with

$$\alpha_{ee} = (l_{\mathrm{eff}}^2/\Delta L)[\omega_m^2 - \omega^2 + 2j\omega/\tau_m], \tag{10a}$$

$$\alpha_{aa} = (A_{\mathrm{eff}}^2/\Delta m)[\omega_e^2 - \omega^2 + 2j\omega/\tau_e], \tag{10b}$$

$$\alpha_{ea} = \alpha_{ae} = l_{\mathrm{eff}} A_{\mathrm{eff}} E_0/\Delta L m, \tag{10c}$$

and where

$$\Delta = \left(\omega_e^2 - \omega^2 + \frac{2j\omega}{\tau_e}\right)\left(\omega_m^2 - \omega^2 + \frac{2j\omega}{\tau_m}\right) - \frac{E_0^2}{Lm}. \tag{11}$$

In this example, the meta-atom responds only to an x-polarized electric field, and, therefore, $\underline{\underline{\alpha}}_{ee}, \underline{\underline{\alpha}}_{ea}, \underline{\underline{\alpha}}_{ae}$ are all scalars. Note the symmetry $\alpha_{ea} = \alpha_{ae}$ as dictated in Eq. (7) by reciprocity. Moreover, assuming that the meta-atom is lossless (namely, only radiation loss is considered), using Eq. (8) we find [37]

$$\begin{aligned} \omega\Im\{\alpha_{ee}^{-1}\}/2 &= P_e^{\mathrm{rad}} + |\alpha_{ae}/\alpha_{ee}|^2 P_a^{\mathrm{rad}}, \\ \omega\Im\{\alpha_{aa}^{-1}\}/2 &= P_a^{\mathrm{rad}} + |\alpha_{ea}/\alpha_{aa}|^2 P_e^{\mathrm{rad}}, \end{aligned} \tag{12}$$

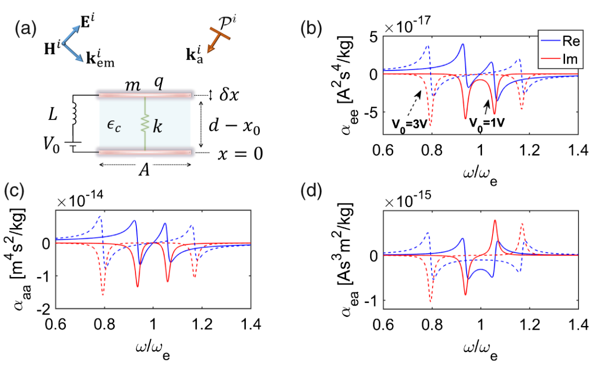

FIG. 2. (a) A parallel plate EMCL meta-atom, set at its operation point by a bias voltage V_0, can be excited by electromagnetic or acoustic fields. Its EMCL small signal (linear) dispersion with frequency is given in (b)–(d). The blue (red) line denotes the real (imaginary) part. The continuous (dashed) line corresponds to biasing voltage $V_0 = 1$ V ($V_0 = 3$ V). (b) The electric polarizability α_{ee}, (c) the acoustic response α_{aa}, the induced acoustic monopole due to a local acoustic pressure field, and (d) the EMCL coupling terms $\alpha_{ae} = \alpha_{ea}$, the induced electric dipole (acoustic monopole) due to a local acoustic pressure (electric) field.

and $\Im\{\alpha_{ee}^*\alpha_{ea}\} = \Im\{\alpha_{aa}^*\alpha_{ae}\} = \Im\{\alpha_{ee}^*\alpha_{aa}\} = 0$. The latter three constraints are related to the mathematical structure of $\underline{\underline{\alpha}}$, whereas the first two constraints, given in Eq. (12), can be solved to find the decay rates τ_e^{-1} and τ_m^{-1}. In the absence of static biasing, $V_0 = 0$, and, therefore, $\alpha_{ae} = \alpha_{ea} = 0$, implying no EMCL coupling. In this case, the relations in Eq. (12) are reduced to the conventional constraint on the polarizability of a small scatterer due to the optical theorem and to its acoustic analog. By plugging Eqs. (10) and (11) into Eq. (12) and solving for τ_e and τ_m, we get

$$\tau_e = \omega^2 L / l_e^2 P_e^{\mathrm{rad}}, \qquad \tau_m = \omega^2 m / A_e^2 P_a^{\mathrm{rad}}. \tag{13}$$

The decay rates are proportional to the radiated power, and, hence, the balance between τ_e and τ_m can be considerably tuned by engineering of the meta-atom ambient medium. Since at a given frequency ω, $\lambda_e = 2\pi c_e/\omega \gg \lambda_a = 2\pi c_a/\omega$, a meta-atom whose typical size is $\sim\lambda_a$ will be electrically deep subwavelength $\ll \lambda_e$. Therefore, typically, the electromagnetic radiation efficiency will be considerably lower than its acoustic counterpart, implying that the electromagnetic resonance dominates since $\tau_e \gg \tau_m$. To change the balance, one may excite higher-order acoustic multipoles that are less efficient radiators or reduce the ambient medium density. However, the greatest control over the meta-atom decay rates will be obtained by placing it in an acoustic or electromagnetic duct or cavity with a suitably engineered local density of states. This idea is demonstrated in Figs. 2(b)–2(d), where the elements of the response matrix are plotted versus the frequency for the meta-atom in Fig. 2(a), with $\omega_e = \omega_m = 2\pi \times 10^6$ rad/s, $A_{\mathrm{eff}} = 3.14\ \mu\mathrm{m}^2$, $l_{\mathrm{eff}} = 10\ \mu\mathrm{m}$, $m = 0.42\ \mu\mathrm{g}$, and $L = 1\ \mu\mathrm{H}$, that is embedded in an electromagnetically transparent, hard-wall acoustic duct with cross section area $A_d = 5A_{\mathrm{eff}}$ that supports an acoustic plane wave only. The mechanical parameters are taken close to Ref. [41]. Here, τ_m is large enough, placing the system in the strong coupling regime. The tunability by the static bias voltage is demonstrated with $V_0 = 1$ and 3 V.

Electrically small direction-of-arrival sensor.—The EMCL meta-atoms discussed above can be used to design piezoelectriclike metamolecules with superior performance due to the joint acoustical and electromagnetic properties. As an interesting example, we design an electrically deep subwavelength, but nevertheless highly sensitive, direction-of-arrival sensor for electromagnetic waves. The system consists of two meta-atoms inside a duct that is centered along the $\hat{y}$ axis and with the same parameters as used for Figs. 2(b)–2(d). We excite the system only by an electromagnetic wave impinging at incidence angle θ_i, so that $\mathbf{U}^i = [E_x^i, 0]^T$ with $E_x^i = E_0 \exp[-jk_e(\cos\theta_i \hat{y} - \sin\theta_i \hat{z})]$ ($k_e = \omega/c_e$). The electric field polarization $\hat{x}$ is normal to the meta-atoms' plates [see Fig. 3(a)]. We set the distance D between the meta-atoms to be electrically deep subwavelength $D \ll \lambda_e$ while acoustically large $D \gg \lambda_a$. The dynamics of the coupled system is given by

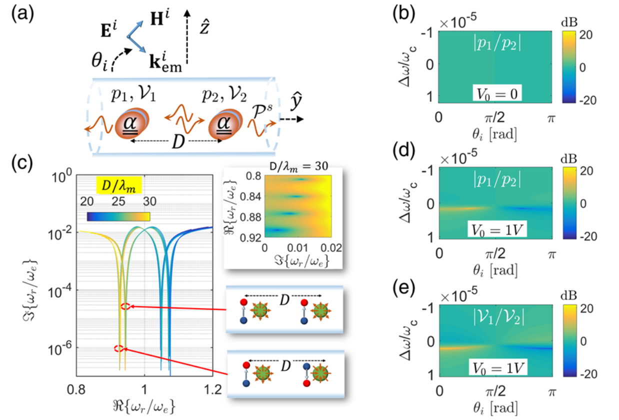

FIG. 3. (a) Illustration of an electrically deep subwavelength direction-of-arrival sensor for an electromagnetic wave. (b) In the absence of EMCL coupling, $V_0 = 0$, only the bright mode can practically be excited, and, therefore, the excitation of the two electric dipoles is practically identical for all θ_i. (c) When the EMCL coupling is turned on, $V_0 = 1$ V, the evolution of the complex eigenfrequencies as the spacing D varies is significant. There are two families of eigenfrequencies corresponding to bright and dark EMCL states. (d) As opposed to (b), here, the electric dipole excitation highly depends on θ_i. (e) Similarly to (d) for the acoustic excitation response.

$$\mathbf{S}_1 = \underline{\underline{\alpha}}[\underline{\underline{G}}(\mathbf{r}_1, \mathbf{r}_2)\mathbf{S}_2 + \mathbf{U}^i(\mathbf{r}_1)],$$
$$\mathbf{S}_2 = \underline{\underline{\alpha}}[\underline{\underline{G}}(\mathbf{r}_2, \mathbf{r}_1)\mathbf{S}_1 + \mathbf{U}^i(\mathbf{r}_2)], \tag{14}$$

where $\mathbf{S}_1$ and $\mathbf{S}_2$ are the EMCL excitation amplitudes of the meta-atoms located at $\mathbf{r}_1 = -D/2\hat{y}$ and $\mathbf{r}_2 = D/2\hat{y}$, respectively. The Green's functions used here are given in Ref. [37]. It is instructive to consider the corresponding eigenvalue problem alongside the excitation one. To find the eigenfrequencies ω_r, we set $\mathbf{U}^i = 0$ and require nontrivial solutions in Eq. (14). In the absence of the EMCL coupling, the system reduces to a simple coupled dipole that supports two resonances, bright and dark, with eigenfrequencies nearly independent of $D \ll \lambda_e$. In this case, an impinging electromagnetic plane wave cannot practically excite the dark mode but only its bright counterpart. Figure 3(b) shows the ratio $|p_1/p_2|$ (in the log scale) as a function of the incidence angle θ_i and the normalized frequency $\Delta\omega/\omega_c$ (where $\Delta\omega = \omega - \omega_c$), around the dark resonance ω_c. Even near the dark resonance $\omega_c = 0.985\,458\omega_m$, there is neither a practical difference between the excitation amplitudes of the dipoles nor any effect when varying the incidence angle θ_i. Here, as opposed to a conventional direction-of-arrival sensor with two antennas separated by $D \sim \lambda_e/2$ [1], the phase difference between the received signals in the two antennas $\sim k_e D$ is extremely small, since $D \ll \lambda_e$. However, we boost the small phase effect by utilizing the presence of EMCL coupling. Since the structure is acoustically large, the number of eigenfrequencies significantly increases, and their complex values strongly depend on D. A typical complex-ω plane showing the resonance locations is given in the inset at the right-upper corner in Fig. 3(c) for $D/\lambda_m = 30$, where $\lambda_m = 2\pi c_a/\omega_m$. In Fig. 3(c), the loci of several complex eigenfrequencies are plotted with D as a parameter whose value is color encoded ($\Im\{\omega_r\}$ is in the log scale to emphasize the resonance's distinct locations). There are two families of eigenfrequencies that correspond to a number of bright and dark modes (see the insets). As an example, we set $D = 28\lambda_m \approx 9.24$ mm and find low loss dark resonance at $\omega_c = 0.928\,46\omega_m$. Remarkably, when exciting the structure with an electromagnetic plane wave at frequencies around the dark resonance, the dark and bright resonances interplay, giving rise to a very strong variation of the excitation amplitudes as a function of the incidence angle θ_i, as shown in Figs. 3(d) and 3(e); as opposed to Fig. 3(b), this is in the presence of EMCL coupling. This correlation can be used to estimate the direction of arrival. Moreover, in this electrically small EMCL sensor scheme, a measurement of the excited acoustic field, as opposed to of the electromagnetic field that can be overwhelmed by the impinging wave, may increase the detection sensitivity and noise fidelity.

Conclusions.—Here, we discussed a paradigm for piezoelectriclike metamaterial building blocks and explored their scattering properties based on first principles. We demonstrated that, using these artificial materials, one can design electrically small devices that are nevertheless highly sensitive to the small electromagnetic-wave phase variation along them. Utilizing this scheme, we designed an electrically deep subwavelength direction-of-arrival sensor. Our results pave the way for a plethora of exciting dynamics and phenomena with potential technological implications in superresolution imaging, miniaturized detectors, electrically small nonreciprocal antennas, and more.

The Tel-Aviv University Rector Startup Fund is acknowledged.

*hadady@eng.tau.ac.il

[1] C. A. Balanis, *Modern Antenna Handbook* (Wiley, New York, 2008).
[2] J. D. Jackson, *Classical Electrodynamics* (Wiley, New York, 1998).
[3] M. Born and E. Wolf, *Principles of Optics* (Cambridge University Press, Cambridge, United Kingdom, 2002).
[4] *Metamaterials: Physics and Engineering Explorations*, edited by N. Engheta and R. W. Ziolkowski (Wiley-IEEE, New York, 2006).
[5] *Theory and Phenomena of Metamaterials*, edited by F. Capolino (CRC Press, Boca Raton, FL, 2009).
[6] Y. Mazor and Ben Z. Steinberg, Metaweaves: Sector-Way Nonreciprocal Metasurfaces, Phys. Rev. Lett. **112**, 153901 (2014).
[7] T. Kodera, D. L. Sounas, and C. Caloz, Magnetless nonreciprocal metamaterial (MNM) technology: Application to microwave components, IEEE Trans. Microwave Theory Tech. **61**, 1030 (2013).
[8] R. Fleury, D. L. Sounas, C. F. Sieck, M. R. Haberman, and A. Alù, Sound isolation and giant linear nonreciprocity in a compact acoustic circulator, Science **343**, 516 (2014).
[9] A. B. Khanikaev, R. Fleury, S. H. Mousavi, and A. Alù, Topologically robust sound propagation in an angular-momentum-biased graphene-like resonator lattice, Nat. Commun. **6**, 8260 (2015).
[10] Y. Hadad, D. L. Sounas, and A. Alù, Space-time gradient metasurfaces, Phys. Rev. B **92**, 100304 (2015).
[11] Y. Hadad, J. C. Soric, and A. Alù, Breaking temporal symmetries for emission and absorption, Proc. Natl. Acad. Sci. U.S.A. **113**, 3471 (2016).
[12] C. Coulais, D. Sounas, and A. Alù, Static non-reciprocity in mechanical metamaterials, Nature (London) **542**, 461 (2017).
[13] K. Fan and Willie J. Padilla, Dynamic electromagnetic metamaterials, Mater. Today **18**, 39 (2015).
[14] N. I. Zheludev and E. Plum, Reconfigurable nanomechanical photonic metamaterials, Nat. Nanotechnol. **11**, 16 (2016).
[15] H. Tao, A. C. Strikwerda, K. Fan, W. J. Padilla, X. Zhang, and R. D. Averitt, Reconfigurable Terahertz Metamaterials, Phys. Rev. Lett. **103**, 147401 (2009).
[16] J. Ou, E. Plum, L. Jiang, and N. I. Zheludev, Reconfigurable photonic metamaterials, Nano Lett. **11**, 2142 (2011).
[17] D. Chicherin, S. Dudorov, D. Lioubtchenko, V. Ovchinnikov, S. Tretyakov, and A. V. Räisänen, MEMS-based high impedance surfaces for millimeter and submillimeter wave applications, Microwave Opt. Technol. Lett. **48**, 2570 (2006).
[18] T. Hand and S. Cummer, Characterization of tunable metamaterial elements using MEMS switches, IEEE Antenna Wireless Prop. Lett. **6**, 401 (2007).
[19] W. M. Zhu *et al.*, Switchable magnetic metamaterials using micromachining processes, Adv. Mater. **23**, 1792 (2011).
[20] J. Valente, J. Ou, E. Plum, I. J. Youngs, and N. I. Zheludev, Reconfiguring photonic metamaterials with currents and magnetic fields, Appl. Phys. Lett. **106**, 111905 (2015).
[21] R. Zhao, P. Tassin, T. Koschny, and C. M. Soukoulis, Optical forces in nanowire pairs and metamaterials, Opt. Express **18**, 25665 (2010).
[22] A. Karvounis, J. Y. Ou, W. Wu, K. F. MacDonald, and N. I. Zheludev, Nano-optomechanical nonlinear dielectric metamaterials, Appl. Phys. Lett. **107**, 191110 (2015).
[23] M. Lapine, I. V. Shadrivov, D. A. Powell, and Y. S. Kivshar, Magnetoelastic metamaterials, Nat. Mater. **11**, 30 (2012).
[24] M. Eichenfield, J. Chan, R. M. Camacho, K. J. Vahala, and O. Painter, Optomechanical crystals, Nature (London) **462**, 78 (2009).
[25] M. Schmidt, V. Peano, and F. Marquardt, Optomechanical metamaterials: Dirac polaritons, Gauge fields, and instabilities, arXiv:1311.7095.
[26] H. Pfeifer, T. Paraso, L. Zang, and O. Painter, Design of tunable GHz-frequency optomechanical crystal resonators, Opt. Express **24**, 11407 (2016).
[27] M. Schmidt, M. Ludwig, and F. Marquardt, Optomechanical circuits for nanomechanical continuous variable quantum state processing, New J. Phys. **14**, 125005 (2012).
[28] V. Peano, C. Brendel, M. Schmidt, and F. Marquardt, Topological Phases of Sound and Light, Phys. Rev. X **5**, 031011 (2015).
[29] E. Buks and M. L. Roukes, Electrically tunable collective response in a coupled micromechanical array, J. Microelectromech. Syst. **11**, 802 (2002).
[30] R. Lifshitz and M. C. Cross, Response of parametrically driven nonlinear coupled oscillators with application to

micromechanical and nanomechanical resonator arrays, Phys. Rev. B **67**, 134302 (2003).

[31] M. Ludwig and F. Marquardt, Quantum Many-Body Dynamics in Optomechanical Arrays, Phys. Rev. Lett. **111**, 073603 (2013).

[32] S. Y. Shah, M. Zhang, R. Rand, and M. Lipson, Master-Slave Locking of Optomechanical Oscillators over a Long Distance, Phys. Rev. Lett. **114**, 113602 (2015).

[33] M.-Ali Miri, E. Verhagen, and A. Alù, Optomechanically induced spontaneous symmetry breaking, Phys. Rev. A **95**, 053822 (2017).

[34] F. Ruesink, M.-Ali Miri, A. Alù, and E. Verhagen, Nonreciprocity and magnetic-free isolation based on optomechanical interactions, Nat. Commun. **7**, 13662 (2016).

[35] M.-Ali Miri, F. Ruesink, E. Verhagen, and A. Alù, Optical Nonreciprocity Based on Optomechanical Coupling, Phys. Rev. Applied **7**, 064014 (2017).

[36] L. E. Kinsler and A. R. Frey, *Fundamentals of Acoustics*, 2nd ed. (Wiley, New York, 1962).

[37] See Supplemental Material at http://link.aps.org/supplemental/10.1103/PhysRevLett.120.054301 for derivation of the main analytical results in the main text.

[38] G. N. Lewis, A new principle of equilibrium, Proc. Natl. Acad. Sci. U.S.A. **11**, 179 (1925).

[39] L. Onsager, Reciprocal Relations in Irreversible Processes, I, Phys. Rev. **37**, 405 (1931).

[40] A. D. Pierce, *Acoustics—An Introduction to Its Physical Principles and Applications*, 3rd ed. (Acoustical Society of America, Melville, NY, 1991), pp. 161 and 319.

[41] P.-L. Yu, T. P. Purdy, and C. A. Regal, Control of Material Damping in High-q Membrane Microresonators, Phys. Rev. Lett. **108**, 083603 (2012).